Design and Analysis of a High-Speed Claw Pole Motor with Soft Magnetic Composite Core

Yunkai Huang, Jianguo Zhu, *Senior Member, IEEE*, Youguang Guo, *Senior Member, IEEE*, Zhiwei Lin, and Qiansheng Hu

***Abstract*—Soft Magnetic Composite (SMC) material is formed by surface-insulated iron powder particles, generating unique properties like magnetic and thermal isotropy, and very low eddy currents. This paper presents the design and analysis of a high-speed claw pole motor with an SMC stator core for reducing core losses and cost. The analyses of magnetic and thermal fields are conducted based on a comprehensive understanding of the property of SMC materials. The 3D finite element analysis (FEA) is performed for accurate parameter calculation, design optimization and thermal calculation. Because of the importance of core loss in high speed motors, rotational core loss model is employed, and the core losses are coupled directly into thermal calculation by keeping the same hexahedral mesh structure between magnetic field analysis and thermal analysis. Since the rotor modal analysis is very important to high-speed motors, the natural frequencies and mode of the rotor are studied.**

***Index Terms*— Core losses, finite element field analysis, high-speed motors, modal analysis, soft magnetic composite (SMC) materials, thermal analysis.**

I. Introduction

SOFT magnetic composite (SMC) materials are very suitable for application in permanent magnet motors with complex structures, 3D magnetic flux paths, and high operating frequencies, because of their unique properties such as the magnetic and thermal isotropy, low eddy current loss, and suitability for complex net shape manufacturing by highly matured powder metallurgical technology. To investigate the application potential of SMC materials in electrical machines, great efforts have been made to employ SMC in various types of motors, such as the claw pole motor [1, 2], transverse flux motor [3], axial flux motor [4], universal motor [5] and so on. These previous works basically focused on the magnetic isotropy and suitability for complex structures of SMC materials. This paper explores the application of SMC materials in the high frequency area.

Compared with conventional general-purpose motors, the major advantages of high speed motors include smaller size for a given power, higher power and torque densities, smaller moment of inertia, which means faster dynamic response, and direct connection with other high speed mechanical devices without using a gearbox. The operational frequency of high speed motors is normally over 1000 Hz, and even 5000 Hz for super-high speed motors. Within this frequency range, the eddy current loss of SMC is much less than that of the conventional silicon steels, and therefore, SMC is an ideal candidate for the stator core. This paper presents the design and analysis of a high-speed 3-phase 3-stack permanent magnet (PM) claw pole motor with SMC core.

Y.K. Huang and Q.S. Hu are with the School of Electrical Engineering, Southeast University, Nanjing, Jiangsu 210096, P. R. China. (Phone: 86-25-83794169-807; e-mail: huangyunkai@gmail.com; huqs@seu.edu.cn).

J.G. Zhu, Y.G. Guo and Z.W. Lin are with the Faculty of Engineering, University of Technology, Sydney NSW 2007, Australia. (e-mail: joe@eng.uts.edu.au; youguang@eng.uts.edu.au; jacklin@eng.uts.edu.au).

II. Structure

Fig.1 illustrates the topology of one of the three stacks of the high speed three phase claw pole PM motor. The stator consists of the claws, the yoke and the coil, and the rotor is simply made of a ring PM magnetized in four poles plus a steel shaft. The three stator stacks are shifted for 120° electrical. Fig.2 shows the dimensional parameters, which were determined and optimized by the FEA to achieve the maximum winding flux.

III. Magnetic Field Analysis

Taking advantage of the periodical symmetry, only one pole pitch region of the machine needs to be calculated. At the two radial boundary planes, the magnetic scalar potential obeys the half-periodical boundary conditions.

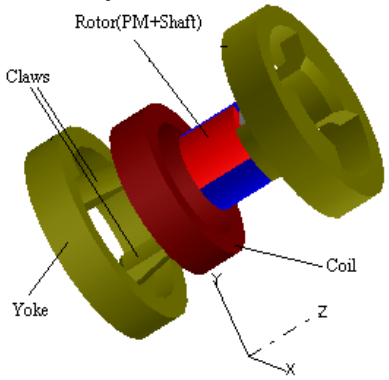

Fig. 1 Magnetically relevant parts of one stack of three phase claw pole motor

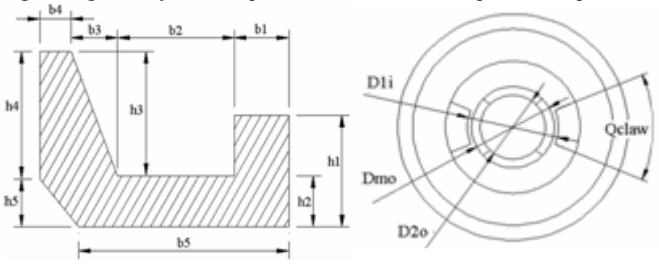

Fig. 2. Dimensional parameters

Above all, the objective of the magnetic field analysis is to determine the dimension of the motor. For example, if the claw pole arc (*Qclaw*, as shown in Fig. 2) increases, the magnetic reluctance of magnetic circuit decreases and hence the winding flux may increase. However, if *Qclaw* is too big, the leakage flux between claw poles would become significant and the winding flux would decrease. Through calculation, as shown in Fig. 3, the winding flux (per turn) achieves the maximum value when *Qclaw* is about 75° electrical. Table I tabulates the dimensions determined through FEA.

Another objective of the magnetic field analysis is to calculate the parameters, such as the EMF, torque, inductance, and core loss. The core loss calculation is crucial for high-speed motors because it is the dominant component of power loss due to high operating frequency. An accurate model including the rotational core loss described in [6] is employed to predict the core loss in the 3D-flux SMC motor. The total core loss is computed based on the time-stepping finite element analysis by separating the hysteresis, eddy current, and anomalous losses in each element under the alternating and rotational magnetic fields.

If the magnetic flux density is sinusoidal, the alternating core loss is calculated by:

$$P_{alt} = K_{ah} f B_m^{\ h} + K_{ae} (f B_m)^2 + K_{aa} (f B_m)^{3/2} \quad \text{(W/kg)} \quad (1)$$

and the core loss with circular rotational flux density by:

$$P_{rot} = P_{rh} + K_{re} (f B_m)^2 + K_{ra} (f B_m)^{3/2} \quad \text{(W/kg)} \quad (2)$$

where

$$\frac{P_{rh}}{f} = a_1 \left[\frac{1/s}{(a_2 + 1/s)^2 + a_3^2} - \frac{1/(2-s)}{[a_2 + 1/(2-s)]^2 + a_3^2} \right]$$

and $$s = 1 - \frac{B_m}{B_s} \sqrt{1 - \frac{1}{a_2^2 + a_3^2}} \quad (3)$$

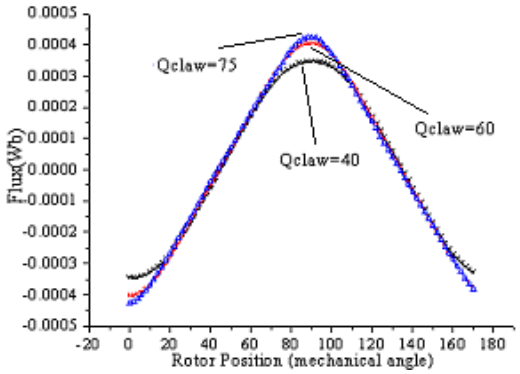

Fig. 3 Winding flux waveform in different *Qclaw*

TABLE I
MAIN DIMENSIONS OF THE MOTOR

Parameter	Value (mm)	Parameter	Value (mm)
b1	7.5	*b2*	7
b3	3	*b4*	2
h1	13	*h2*	6.6
h3	16.4	*h4*	20
h5	3	*D2o*	20
Dmo	26	*D1i*	28

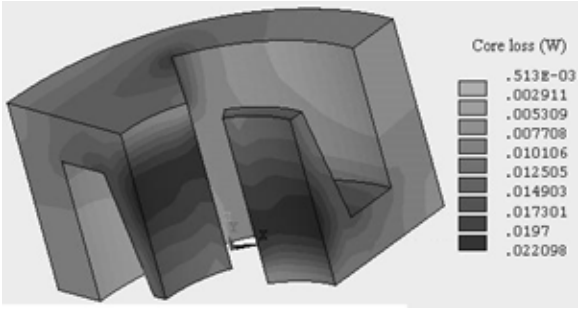

Fig. 4 Core loss distribution at no-load

The coefficients K_{ah}, h, K_{ae}, K_{aa}, K_{re}, K_{ra}, a_1, a_2, a_3 and B_s can be deduced from the data measured by the rotational core loss tester, and B_m is the peak value of sinusoidal flux density.

The core loss with elliptical ***B*** is predicted from the alternating and circularly rotating core losses by:

$$P_{fe} = R_B P_{rot} + (1 - R_B)^2 P_{alt} \quad \text{(W/kg)} \quad (4)$$

where $R_B = B_{min}/B_{maj}$ is the axis ratio, and B_{maj} and B_{min} are the major and minor axes of the elliptical ***B*** locus. The distribution of stator core loss at no-load (30 krpm) is shown in Fig. 4. The core loss in the claws is greater than that in other parts of stator core because the changing amplitude of magnetic filed is greater than that in other parts.

IV. THERMAL FIELD ANALYSIS

A thermal network method used in claw pole motor is described in [7]. The whole motor is divided into many small solid cubic elements, which can be modeled by six thermal resistances and seven nodes. But the core loss of each element in thermal network cannot be obtained readily from the result of magnetic filed calculation. Mostly, the average is used. Because the core loss distribution is quite different in different position of the stator core, the accuracy cannot be improved by increasing the number of elements in thermal network. In this paper, 3D finite element thermal analysis is used to analyze the temperature distribution. Ignoring the heat transfer by radiation, we can express the partial differential equation governing the heat conduction and convection as:

$$\rho c \left(\frac{\partial T}{\partial t} + \{V\}^T \{L\} T \right) = \{L\}^T ([D]\{L\}T) + Q \quad (5)$$

where ρ (Kg/m^3) is the mass density, c (J/KgK) the specific h eat, T (K) the temperature, t (s) the time,

$$\{L\} = \begin{Bmatrix} \frac{\partial}{\partial x} \\ \frac{\partial}{\partial y} \\ \frac{\partial}{\partial z} \end{Bmatrix}, \quad \{V\} = \begin{Bmatrix} V_x \\ V_y \\ V_z \end{Bmatrix} \text{ and } [D] = \begin{bmatrix} K_{xx} & 0 & 0 \\ 0 & K_{yy} & 0 \\ 0 & 0 & K_{zz} \end{bmatrix}$$

are the vector partial differential operator, the velocity vector for mass transport of heat, and the conductivity matrix, K_{xx}, K_{yy}, and K_{zz} (W/mK) the thermal conductivity along the x, y, and z directions, respectively, and Q (W/m^3) is the heat generation rate per unit volume.

In steady-state, the temperature does not vary with time, and

the first term in the left-hand side of (5) becomes zero. Each element's core loss calculated from magnetic field analysis is applied as the body loads to the corresponding element in thermal analysis by keeping the same size and number of element. The boundary conditions can be of Dirichlet type, where the temperature T* on the boundary is specified. This boundary condition can be applied to the surface between the frame and outer air.

A Neumann type of boundary condition specifies the heat flux flow q_n through a boundary. Newton's convection boundary condition is:

$$q_n = n \bullet (k\nabla T) = \alpha(T - T_{amb}) \qquad (6)$$

The heat flux flow through the boundaries to the surrounding is described with the heat transfer coefficient α and the ambient temperature T_{amb}. The convective heat transfer to the surroundings is dependent on the geometry and the cooling conditions. The air gap convection coefficient is determined by two main quantities: the ruggedness of the rotor and stator surfaces and the peripheral speed of the rotor surface. By assuming smooth surfaces, the convection coefficient can be calculated by experiential formulae [8]:

$$\alpha_\delta = 28(1+\omega_\delta{}^{0.5}) \qquad (\mathrm{W/(m^2*K)} \qquad (7)$$

and

$$\omega_\delta = \sqrt{(0.5v_r)^2 + v_a{}^2} \qquad (\mathrm{m/s}) \qquad (8)$$

where v_r and v_a are the peripheral and axial speed of the rotor surface, respectively.

Other losses, such as the copper loss and air friction loss, are also applied to the model as body loads. The temperature distribution at no-load is shown in Fig. 5. The temperature is affected by the core loss mainly because it is greater than other losses in high-speed motor. The core temperature is fine, because the rated temperature of motor is 75 Celsius degrees, and the maximum temperature of the insulating material and magnet is 100 Celsius degrees.

V. Rotor Modal Analysis

Accurate prediction of the natural frequencies and modes of the rotor at the design stage is clearly critical, since an inappropriate rotor design may lead to excessive acoustic noise emissions, excessive bearing loss, and even catastrophic failure. The finite element analysis is used to investigate the influence of design parameters on the natural frequencies. The rotor consists of a steel shaft, PMs and two bearings. In the finite element analysis, the bearings are modeled as springs. As shown in Fig.6, four springs are used for each bearing to ensure that the rotor shaft is supported evenly. Table II presents the calculation results.

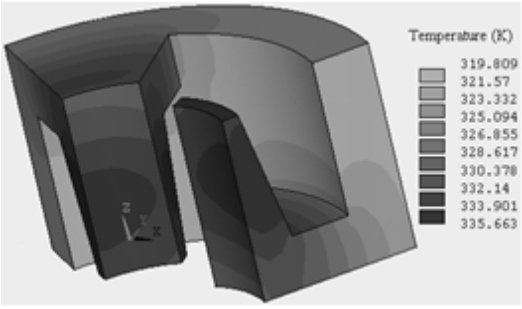

Fig. 5 The temperature distribution in stator core (K)

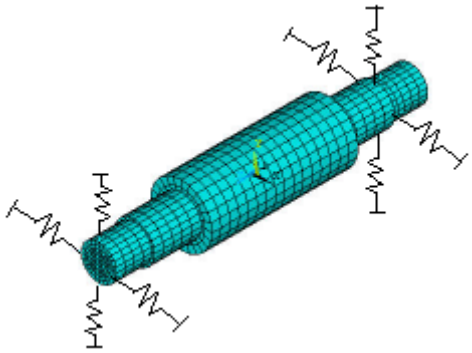

Fig. 6 FE model of rotor with bearings

TABLE II
NATURAL FREQUENCIES OF ROTOR

Mode	Frequency (Hz)
1st bending	2820
2nd bending	7715
3rd bending	10424

From the sensitivity study, the bearing stiffness, the shaft length, the shaft diameter and the position of bearing have significant influence on the rotor natural frequency. In order to lift rotor natural frequency beyond the operating speed range, the shaft should be short and have a large diameter.

VI. Conclusion

In this paper, the magnetic, thermal and modal analyses have been conducted on a high-speed three phase claw pole PM motor with SMC core by using 3D finite element analysis. The core loss is calculated by rotational core loss model, and it is coupled directly into the thermal finite element analysis, so that accurate temperature distribution can be obtained. This is very important in high-speed motor design.

References

[1] Y. G. Guo, J. G. Zhu, P. A. Watterson, W. M. Holliday, and W. Wu, "Improved design and performance analysis of a claw pole permanent SMC motor with sensorless brushless DC drive," Power Electronics and Drive Systems, 2003. PEDS 2003. The Fifth International Conference on, vol. 1, pp. 704-709.

[2] J. Cros and P. Viarouge, "New structures of polyphase claw-pole machines," Industry Applications Conference, 2002. 37th IAS Annual Meeting. , vol. 4, pp. 2267 - 2274

[3] Y. G. Guo, J. G. Zhu, P. A. Watterson, and W. Wu, "Development of a PM transverse flux motor with soft magnetic composite core," *Energy Conversion, IEEE Transactions on*, vol. 21, pp. 426-434, 2006.

[4] Y. Chen and P. Pillay, "Axial-flux PM wind generator with a soft magnetic composite core," Industry Applications Conference, 2005. Fourtieth IAS Annual Meeting, vol. 1, pp. 231-237.

[5] J. Cros, P. Viarouge, Y. Chalifour, and J. Figueroa, "A new structure of universal motor using soft magnetic composites," *Industry Applications, IEEE Transactions on*, vol. 40, pp. 550-557, 2004.

[6] J. G. Zhu and V. S. Ramsden, "Improved formulations for rotational core losses in rotating electrical machines," *IEEE Trans. On Magnetics*, vol. 34, pp. 2234-2242, July 1998.

[7] Y. G. Guo, J. G. Zhu, and W. Wu, "Thermal analysis of soft magnetic composite motors using a hybrid model with distributed heat sources," *Magnetics, IEEE Transactions on*, vol. 41, pp. 2124-2128, 2005.

[8] Y. T. Wei, D. W. Meng, and J. B. Wen, *The heat transfer in electrical machines*. Beijing: China mechanism publisher, 1998.